CrossMark

ORIGINAL ARTICLE

High-rate clock variations of the Galileo IOV-1/2 satellites and their impact on carrier tracking by geodetic receivers

O. Montenbruck[1] · A. Hauschild[1] · S. Häberling[2] · B. Braun[1] · G. Katsigianni[3] · U. Hugentobler[3]

Abstract The carrier signals of the first two Galileo satellites, IOV-1 and IOV-2, exhibit subtle phase variations, which may cause high-rate oscillations in carrier phase measurements of geodetic-grade receivers as well as associated Doppler measurement errors. The carrier phase oscillations slightly exceed the noise level of the measurements and have been attributed to a subtle cross talk of signals from two active atomic frequency standards in the clock monitoring and control unit (CMCU). This cross talk is only present in the first two IOV satellites, and its practical implications have partly been compensated by now through a suitable configuration of the CMCU. Nevertheless, a proper understanding of the phenomenon is deemed relevant to the interpretation of Galileo IOV measurements collected with global ground networks in the 2012 to early 2015 time frame. Also, the data collected so far offer valuable insight into the tracking of high-frequency signal variation of geodetic receivers that are of interest for applications such as structural monitoring or earthquake research. We present practical measurements from zero-baseline tests of common geodetic receivers with data rates of 1/30–1 Hz as well as dedicated tests with high-rate (50–100 Hz) receivers to evidence the phenomenon. Efforts are made to understand the different response of specific receivers based on generic receiver tracking and measurement generation concepts.

Keywords Galileo · Clock oscillation · CMCU

Introduction

Within the multi-GNSS experiment (MGEX; Montenbruck et al. 2014) network of the International GNSS Service (IGS), various sites are equipped with pairs of geodetic receivers connected to a common antenna. These offer a convenient "zero-baseline" testbed for characterizing receiver noise and intersystem biases of the new GNSS signals and constellations. As part of such tests, oscillatory variations of sub-centimeter amplitude and periods of about 4 min have been identified by various researchers in double-difference carrier phase observations of the first Galileo in-orbit validation (IOV) satellites. In parallel, periodic errors in Doppler with amplitudes at the decimeter-per-second level have been reported in Borio et al. (2015). The oscillations are limited to the first two IOV satellites and mainly affect observations collected before 2015. No such phenomena were observed on the IOV-3/4 satellites or the full operational capability (FOC) satellites.

The aforementioned effects have been attributed to a cross talk between the two frequency synthesizers of the clock monitoring and control unit (CMCU; Felbach et al. 2003; Carrillo et al. 2005; Felbach et al. 2010) along with an intentional misalignment of the respective frequencies. We therefore start this analysis with an overview of the CMCU and provide a simple model to describe the impact of a cross talk between two frequency sources on the transmitted signal and the measured carrier phase. Next, high-rate receiver data are presented which provide the

✉ O. Montenbruck
oliver.montenbruck@dlr.de

[1] Deutsches Zentrum für Luft- und Raumfahrt, German Space Operations Center, Oberpfaffenhofen, Germany

[2] Eidgenössische Technische Hochschule, Institut für Geodäsie und Photogrammetrie, Zurich, Switzerland

[3] Technische Universität München, Inst. für Astronomische und Physikalische Geodäsie, Munich, Germany

Springer

most direct evidence of the oscillations but also illustrate differences in the tracking and measurement formation by today's multi-GNSS receivers. Finally double-difference observations from the zero-baseline testbeds are presented to describe the impact of the IOV-1/2 signal characteristics on geodetic measurements and to discuss their implications for Galileo IOV-1/2 precise orbit and clock determination as well as precise point positioning and relative navigation. Complementary to carrier phase measurements, which are most widely used in high-precision applications, the impact of the IOV-1/2 signal on Doppler measurements is discussed, which are mainly used for single-point velocity estimation in mobile receivers. It is shown that the receiver response to the periodic signal variation is highly dependent on the receiver architecture and configuration.

CMCU and signal model

As introduced above, the IOV signal oscillations have been related to a cross talk in the clock monitoring and control unit (CMCU) of the Galileo satellites, which is schematically shown in Fig. 1 (Felbach et al. 2003; Carrillo et al. 2005). In total, the Galileo IOV satellites are equipped with four atomic clocks, namely two passive hydrogen masers (PHMs) and two rubidium atomic frequency standards (RAFSs). At any time, two of these clocks are operated in a hot redundant configuration, while the other two serve as cold redundant backup. The clocks generate a native signal of 10 MHz (RAFS) or 10.0028 MHz (PHM), which is mixed with a digitally generated 230 kHz signal to obtain the master clock frequency $f_0 = 10.23$ MHz from which all carriers and the modulation of the navigation signal are derived. The synthesizer can be controlled to fine-tune the resulting frequency with a resolution of 5.55×10^{15}. To
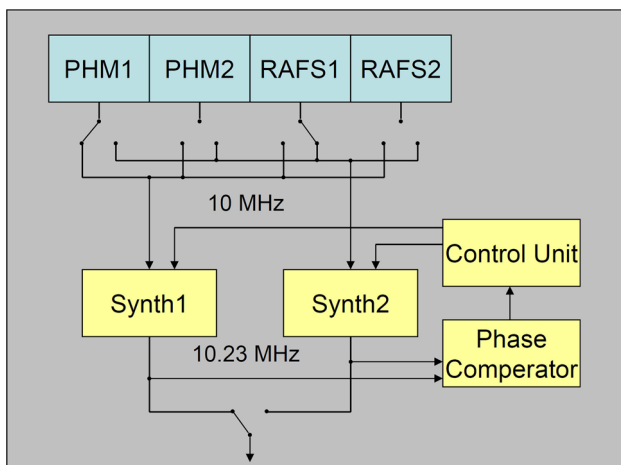
enable a hot swap, the outputs of two synthesizers connected to the two active clocks are continuously compared and can thus be aligned with each other. One output is then selected for the master signal.

In case of IOV-1/2, a subtle leakage of signals occurs between the two synthesizer chains resulting in superposition of the master signal with a small fraction of the secondary chain. Based on an operational decision, a frequency offset of $\delta f \approx 5.996$ Hz had been configured between both synthesizers after revealing the cross talk in the initial in-orbit testing.

Given a nominal amplitude A and a cross-coupling factor α, the combined clock signal as a function of time t can be described as

$$s(t) = A \cdot e^{2\pi j f_0 t} + \alpha A \cdot e^{2\pi j ((f_0 + \delta f)t + \delta \phi_0)} \tag{1}$$

where f_0 denotes the frequency of the primary signal, while δf and $\delta \phi_0$ are the frequency and initial phase offset of the leaked signal component from the second synthesizer (Fig. 2). For sufficiently small values of α, this translates into

$$s(t) = (1 + \alpha \cos(\delta \phi)) \cdot e^{j\alpha \sin(\delta \phi)} \cdot A \cdot e^{2\pi j f_0 t} \tag{2}$$

with

$$\delta \phi = 2\pi \delta f t + \delta \phi_0 \tag{3}$$

Compared to the nominal signal, the signal with cross talk exhibits a periodic amplitude and phase variation, where the period is given by the inverse of the frequency difference of the two synthesizers and where the amplitude and phase variation are proportional to the cross-coupling ratio α.

The periodic clock phase variation translates into a time offset

$$\delta t(t) = \frac{\alpha \sin(\delta \phi)}{2\pi f_0} \tag{4}$$

of the master clock and corresponds to a periodic range variation

$$\delta \rho(t) = \alpha \left[\frac{c}{2\pi f_0} \right] \sin(2\pi \delta f t + \delta \phi_0) \tag{5}$$

where c denotes the speed of light and where the term in brackets amounts to about 4.7 m. Equation (5) applies under the assumption that the carrier signals transmitted by

Fig. 1 Overview of the Galileo IOV 10.23 MHz clock signal generation (adapted from Felbach et al. 2003; Carrillo et al. 2005)
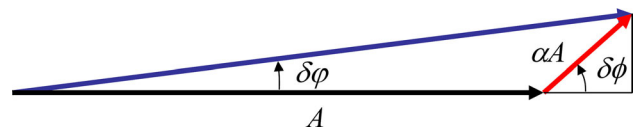

Fig. 2 Phasor diagram illustrating the superposition of the primary and cross talk clock signals

the IOV satellites are obtained by mixing the CMCU output with integer multiples of a clean 10.23 MHz signal, so that all resulting carrier signals would show the same frequency δf and amplitude $\delta \rho(t)$ of the clock oscillation. As further discussed below, this is indeed consistent with actual observations of the clock variation on E1 and E5a signals. These exhibit amplitudes of about 2–3 mm, which suggest a value of $\alpha \approx 0.5 \times 10^{-3}$ and correspond to a relative power of about -65 dB for the cross talk between the two synthesizers.

Even though the periodic phase variations are accompanied by amplitude variations that are shifted by a quarter period, the amplitude changes are hardly observable and have no practical relevance. Carrier-to-noise density ratio (C/N_0) values of common receivers are typically too noisy to show variations of about 0.002 dB amplitude. In addition C/N_0 measurements are commonly filtered with timescales exceeding the relevant periods. Within the subsequent discussion, focus will therefore be given to carrier phase and Doppler (range-rate) observations.

High-rate measurements

In order to resolve the periodic oscillation in the IOV-1/2 satellites, carrier phase measurements on the E1/L1 and E5a/L5 frequencies were collected with various receivers offering sampling rates of 25–100 Hz. High-elevation observations were considered to maximize signal strength and thus to minimize the impact of thermal noise on the measurements as well as to reduce the impact of tropospheric and ionospheric propagation effects. Furthermore, the measurements were differenced against a reference satellite to rigorously eliminate the receiver clock. Only very short data arcs of typically 10 s are required to monitor the high-rate signal oscillations. A simple detrending using a low-order polynomial is therefore sufficient to remove the geometric range variation as well as satellite clock drifts and atmospheric delay variations. Ideally, the detrended single-frequency, single-difference observations then provide a direct measurement of the periodic carrier variation. In practice, these measurements are also affected by receiver thermal noise and multipath as well as stochastic satellite clock variations for each of the two signals that are used to form the difference. In order to minimize the impact of the latter contribution, satellites with high-grade clocks such as GPS Block IIF satellites or any of the other Galileo IOV/FOC satellites are best suited as reference satellites. These exhibit representative clock stabilities of better than $10^{-12}/\sqrt{\tau/\mathrm{s}}$, which are generally lower than the receiver noise contribution at timescales near $\tau = 1$ s (Griggs et al. 2015).

Selected results obtained with different types of high-rate receivers are illustrated in Fig. 3. In all cases the carrier phase measurements of the IOV-1 or IOV-2 satellite have been differenced against a high-elevation Block IIF GPS satellite and a fourth-order polynomial was used for detrending. While the oscillation of about 6 Hz is easily recognized in the graphs, it is superimposed by measurements errors and stochastic clock variations. For a quantitative analysis of the clock oscillation, a two-parameter least-square fit has therefore been used to adjust the amplitude and phase of a pure sine wave with a given frequency of 5.996 Hz. The resulting amplitudes are summarized in Table 1. Subject to availability of suitable data sets, results for both IOV satellites are given.

Depending on the specific receiver and configuration, amplitudes in the range of 1–4 mm are obtained. The measured clock variations of IOV-2 exhibit only slightly (10–20 %) larger amplitudes than that of IOV-1, indicating that both satellites experience a comparable amount of cross talk.

With the exception of one receiver family, fairly equal amplitudes are measured on the E1 and E5a signals as should be expected for any form of periodic range or clock variation affecting the received signal. It may be noted, though, that different receivers exhibit notably different amplitudes of the measured phase variations. In order to understand this unexpected behavior, attention must be paid to the fact that all carrier phase measurements result from the output of a phase-locked loop (PLL) that is used inside the receiver to continuously align a carrier replica with the incoming signal (Ward et al. 2006). The loop response to time-varying signals depends primarily on the loop order and the loop bandwidth (B), which represents a compromise between the resulting noise and the capability to follow a rapid signal variations (Häberling et al. 2015). While the measurement noise is lower for smaller bandwidths, the tracking loop is more responsive for higher bandwidths.

While details of the loop design remain undisclosed for most receivers, a third-order PLL as discussed in Ward et al. (2006) can be considered as a representative reference to better understand the observed receiver behavior. Its transfer function is given by

$$H(s) = \frac{b\omega_0 s^2 + a\omega_0^2 s + \omega_0^3}{s^3 + b\omega_0 s^2 + a\omega_0^2 s + \omega_0^3} \qquad (6)$$

where the loop parameters are chosen as

$$a = 1.1 \quad \text{and} \quad b = 2.4 \qquad (7)$$

With these values, the characteristic frequency ω_0 [in (rad/s)] and the bandwidth B [in (Hz)] are related by

$$\omega_0 = B/0.7845 \qquad (8)$$

The corresponding expressions for a second-order PLL are given by

Fig. 3 Periodic clock variations of Galileo IOV-1/2 from detrended single-difference carrier phase measurements on the E1 frequency obtained with a Trimble NetR9 receiver (*top*), a Septentrio PolaRx-S receiver (*center*) and a Javad Delta-G3TH receiver (*bottom*). The measured clock variation at 50 or 100 Hz sampling is indicated through red dots connected by a *solid black line*, while the *blue line* reflects an adjusted sine wave of 5.996 Hz
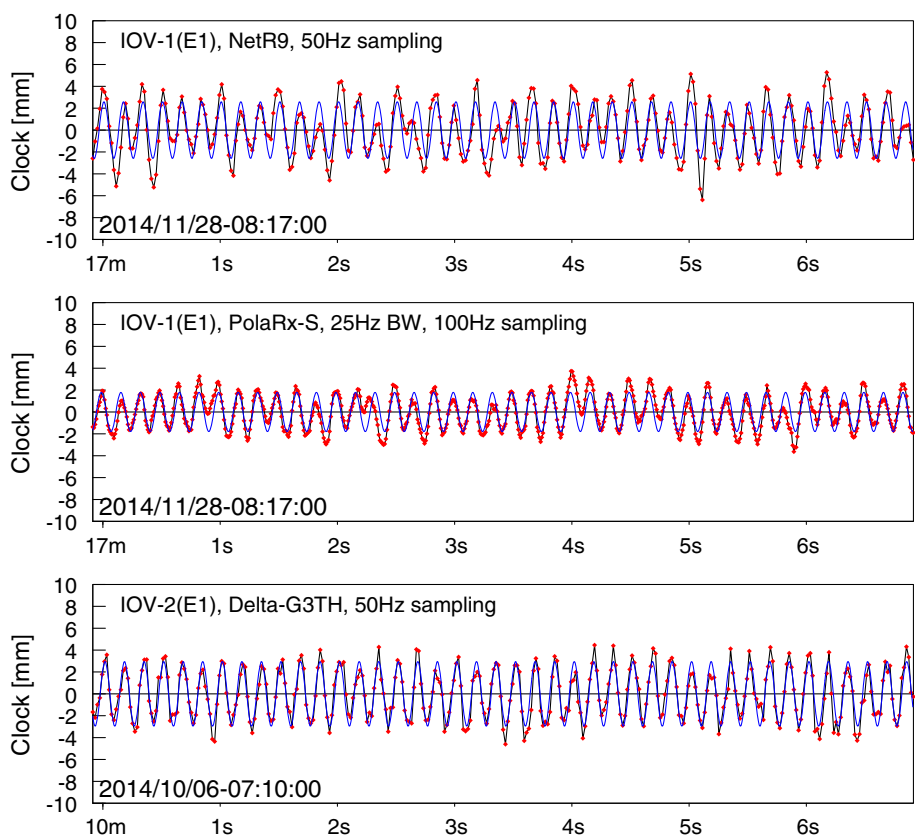
Table 1 Amplitudes of IOV-1/2 clock variations from detrended single-difference carrier phase observations collected over selected 10-s intervals

Receiver	B	Rate	IOV-1		IOV-2	
	(Hz)	(sps)	E1	E5a	E1	E5a
NetR9	–	50	2.6[a]	2.6[a]	3.0[b]	3.0[b]
PolaRx-S	15	100	1.2[a]	1.4[a]	1.5[a]	1.7[a]
	25	100	1.8[a]	2.0[a]	2.2[a]	2.5[a]
Delta-G3TH	25	50	–	–	2.9[b]	4.3[b]
Sigma-G3TAJ	25	100	2.6[c]	4.1[c]	2.8[c]	4.0[c]
	25	20	–	–	2.9[d]	4.2[d]
GRX1200	15	20	–	–	3.1[d]	3.1[d]

All values are given in (mm) and exhibit a repeatability for different data intervals of 1 mm or better

Dashes indicate unavailable data. Where available, the adopted PLL bandwidth (B) of the receiver is specified in the second column

Superscripts indicate the epoch of the respective data ([a] 2014/11/28 08:15; [b] 2014/10/06 07:10; [c] 2013/03/12 11:15; [d] 2014/03/06 10:15)

$$H(s) = \frac{a\omega_0 s + \omega_0^2}{s^2 + a\omega_0 s + \omega_0^2} \tag{9}$$

with $a = \sqrt{2}$ and $\omega_0 = B/0.53$ (Ward et al. 2006).

For a periodic input signal of frequency f, the amplitude and phase response of the PLL can be obtained from

$$A(f) = |H(2\pi jf)| \tag{10}$$

and

$$\Phi(f) = \arctan\left(\frac{\text{Im}[H(2\pi jf)]}{\text{Re}[H(2\pi jf)]}\right) \tag{11}$$

respectively. These values are shown in Fig. 4 for representative PLL bandwidths of 15 and 25 Hz. For comparison, both third- and second-order loops are illustrated, since actual amplitude response measurements provided in Häberling et al. (2015) indicate a better match with the predicted response of a second-order loop for some of their test receivers.

It may be recognized that the clock oscillation of the IOV-1/2 satellites has a frequency that is well outside the range of roughly $f < 1$ Hz in which the input signal passes the loop filter transparently. In the vicinity of the characteristic loop frequency $\omega_0/(2\pi)$, a notable amplification occurs, which is followed by an attenuation that becomes more pronounced as the input frequency increases. Furthermore, the loop filter induces a phase lag which grows with frequency.

The loop characteristics are also reflected in the autocorrelation function of the measured carrier phase data. By way of example, the autocorrelation function of a Javad Sigma-G3TAJ as obtained in a zero-baseline test with two identical receivers is illustrated in Fig. 5. Despite identical bandwidth
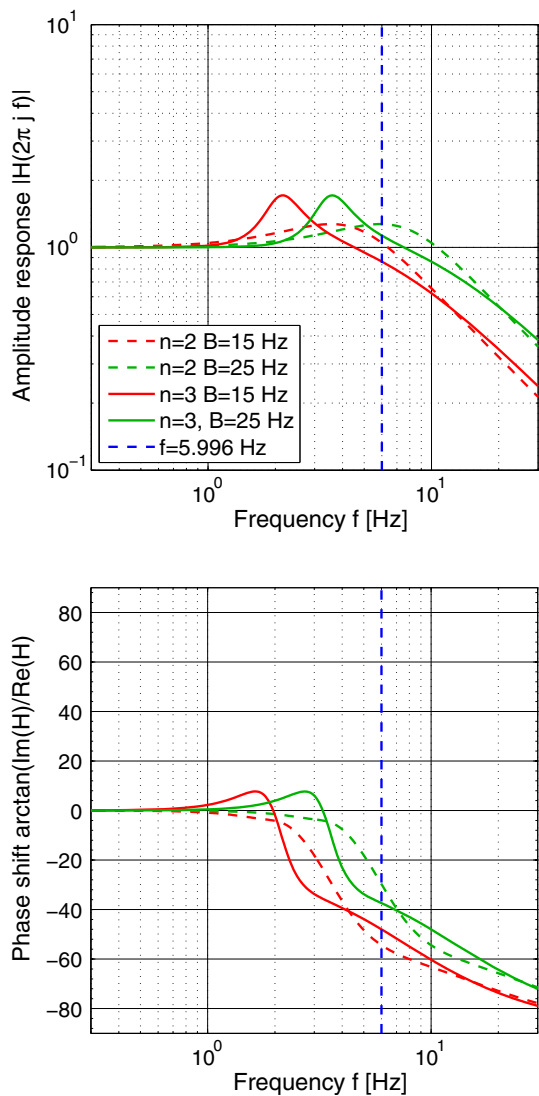
Fig. 4 Amplitude (*top*) and phase response (*bottom*) of second-order ($n = 2$) and third-order ($n = 3$) PLLs with loop parameters of Ward et al. (2006) and different bandwidths. The *dashed blue line* marks the frequency of the IOV-1/2 clock oscillation

Fig. 5 Autocorrelation function of a Javad Sigma-G3TAJ receiver for E1 and E5a signals using common PLL bandwidth settings of $B = 25$ Hz

settings for E1 and E5a tracking, obvious differences in the autocorrelation function may be recognized, which relate to the different amplitudes of the clock oscillation as measured with this receiver on the two frequencies (Table 1).

Even though the tracking loops of all receivers, frequencies and signals experience a common input signal caused by the oscillation of the satellite clock, they may show different phases and amplitudes in the carrier phase measurements due to different characteristics of the employed tracking loops. While a quantitative analysis is beyond the scope and capabilities of the present study, the considerations given above offer at least a qualitative explanation for the varying amplitudes of the observed clock oscillations compiled in Table 1.
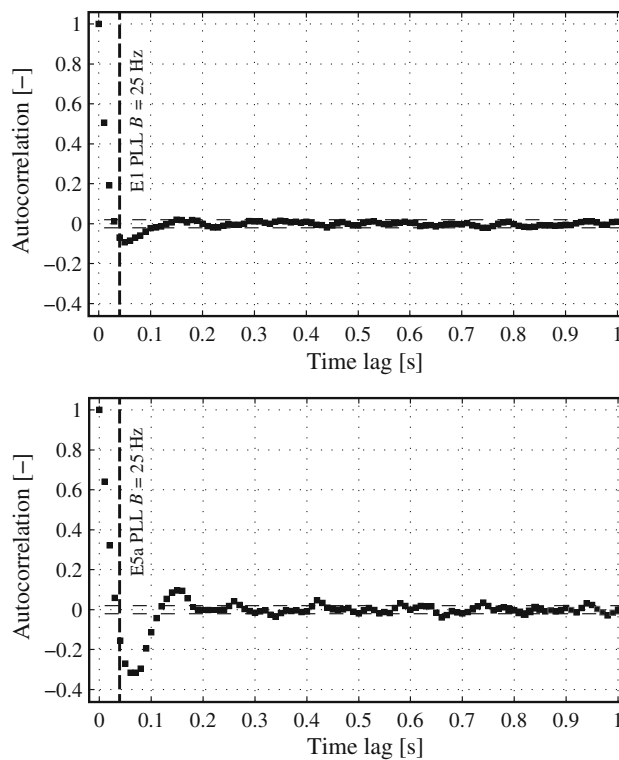
We conclude this section with a brief discussion of high-rate carrier phase measurements of IOV-1/2 collected in March 2015. As illustrated in Fig. 6, no traces of a periodic clock variation could be sensed at this time for the IOV-1 satellite, whereas IOV-2 exhibits oscillations at a much higher frequency of $\delta f \approx 12.59$ Hz. While the figure illustrates the measurements for only a single receiver, similar results were, e.g., obtained with a Leica GR25 receiver at 25 Hz bandwidth and 50 Hz sampling. Obviously, the different signal characteristics with respect to the October/November 2014 time frame reflect the result of a modified CMCU configuration. For IOV-2 the frequency of the resulting clock oscillation has more than doubled but is nevertheless still discernible with high-rate measurements and high PLL bandwidths. In case of IOV-1, a continuous alignment ($\delta f \approx 0$) of both synthesizers is performed since early 2015 to avoid the presence of oscillations in the clock signal (F. J. Gonzalez Martinez, priv. comm.).

Doppler measurements

Aside from carrier phase observations, the IOV-1/2 clock oscillation can also be recognized from Doppler, or (pseudo-)range-rate, measurements (Borio et al. 2015). The instantaneous frequency shift of the received signal can be

Fig. 6 Periodic clock variations of Galileo IOV-1 (*top*) and IOV-2 (*bottom*) from detrended single-difference carrier phase measurements on the E1 frequency obtained with a Javad Delta-G3T receiver in March 2015. The *blue line* reflects an adjusted sine wave of 12.59 Hz and 2.9 mm amplitude
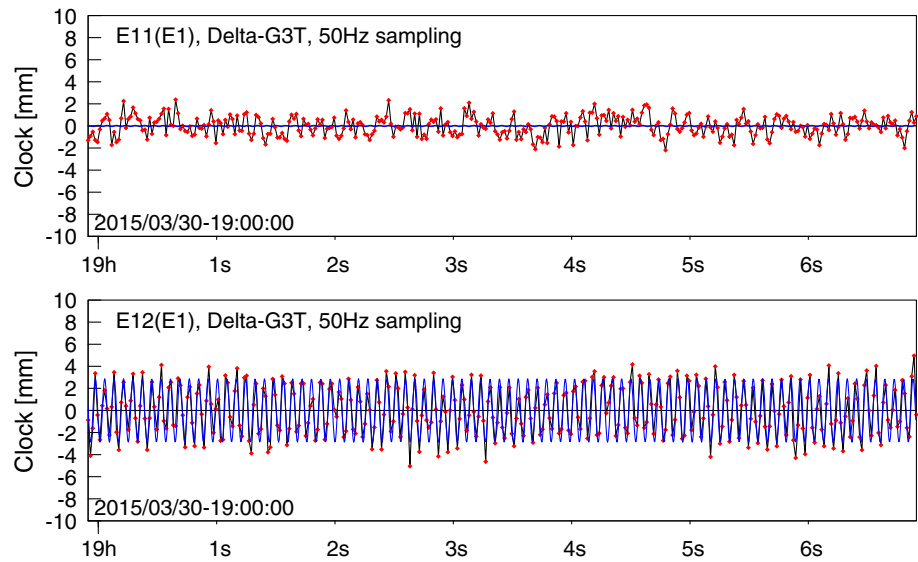
obtained from the rate of the numerically controlled oscillator used to track the incoming carrier in a frequency-locked loop (FLL) or phase-locked loop (PLL). In order to reduce the resulting noise level, it has become common practice, though, to approximate the Doppler/range-rate from time-differenced carrier phase observations. Since a simple difference quotient approximation

$$\dot{\varphi}(t_i) \approx \frac{\varphi(t_i) - \varphi(t_{i-1})}{\Delta t} \tag{12}$$

using two phase measurements separated by $\Delta t = t_i - t_{i-1}$ may cause notable errors for accelerated motion, a polynomial of second order is used in practice to interpolate or adjust the carrier phases and subsequently obtain the desired rate of change by differentiation. Considering three consecutive and equally spaced phase measurements, the resulting range-rate is given by

$$\dot{\varphi}(t_i) \approx \frac{3\varphi(t_i) - 4\varphi(t_{i-1}) + \varphi(t_{i-2})}{2\Delta t} \tag{13}$$

The associated noise amounts to

$$\sigma_{\dot{\varphi}} = \sqrt{\frac{13}{2}} \frac{\sigma_{\varphi}}{\Delta t} \tag{14}$$

and decreases with increasing step size Δt. Millimeter-level carrier phase noise thus translates into centimeter-per-second level range-rate precision when applying time steps of 0.1 s or higher as an alternative to an interpolating polynomial, and an approximating polynomial may be adjusted to a larger set of high-rate phase measurements and differentiated to obtain the phase rate at the current epoch. Irrespective of the specific approach, however, larger time intervals result in improved noise characteristics but may be less suitable to follow rapid signal dynamics.

Considering the 6 Hz carrier phase oscillation in the IOV-1/2 clock signals, an amplitude of $A_{\varphi} \approx 2-3$ mm would result in a nominal amplitude

$$A_{\dot{\varphi}} = 2\pi\delta f \cdot A_{\varphi} \approx 7-11 \text{ cm/s} \tag{15}$$

of the periodic (pseudo)range-rate variation. Results from actual receiver measurements are compiled in Fig. 7 for the test cases previously illustrated in Fig. 3. Numerical values of the amplitudes for the two IOV satellites and a larger set of test cases are, furthermore, collated in Table 2.

While the individual receivers showed a fairly similar amplitude of the carrier phase oscillation, the same does not hold for the associated rates. With one exception, the amplitude of the clock rate variation is substantially smaller than expected from the time derivative of the clock oscillation or even completely absent. This widely different behavior can, most likely, be attributed to the number and spacing of carrier phase samples used to derive the range-rate measurements as well as a possible supplementary filtering. While the NetR9 receiver provides "near-instantaneous" range-rate observations, the PolaRx-S and Delta-G3TH/Sigma-G3TAJ receivers effectively average the actual clock variations over timescales larger than the oscillation period. Different Doppler amplitudes may also be recognized for the test data sets obtained with the Delta-G3TH and Sigma-G3TAJ. Even though both receiver types make use of similar hardware and software components, different Doppler smoothing bandwidths of 0.1 and 3 Hz, respectively, were employed in the two cases.

Depending on the receiver-specific algorithms for the generation of Doppler/range-rate observations, a widely varying impact on the computation of single-point velocity computations may thus be expected. Likewise the efficiency of filtering concepts as suggested in Borio et al.

Fig. 7 Periodic clock rate (Doppler) variations of Galileo IOV-1/2 from detrended single-difference range-rate measurements on the E1 frequency obtained with a Trimble NetR9 receiver (*top*), a Septentrio PolaRx-S receiver (*center*) and a Javad Delta-G3TH receiver (*bottom*) corresponding to the examples shown in Fig. 3
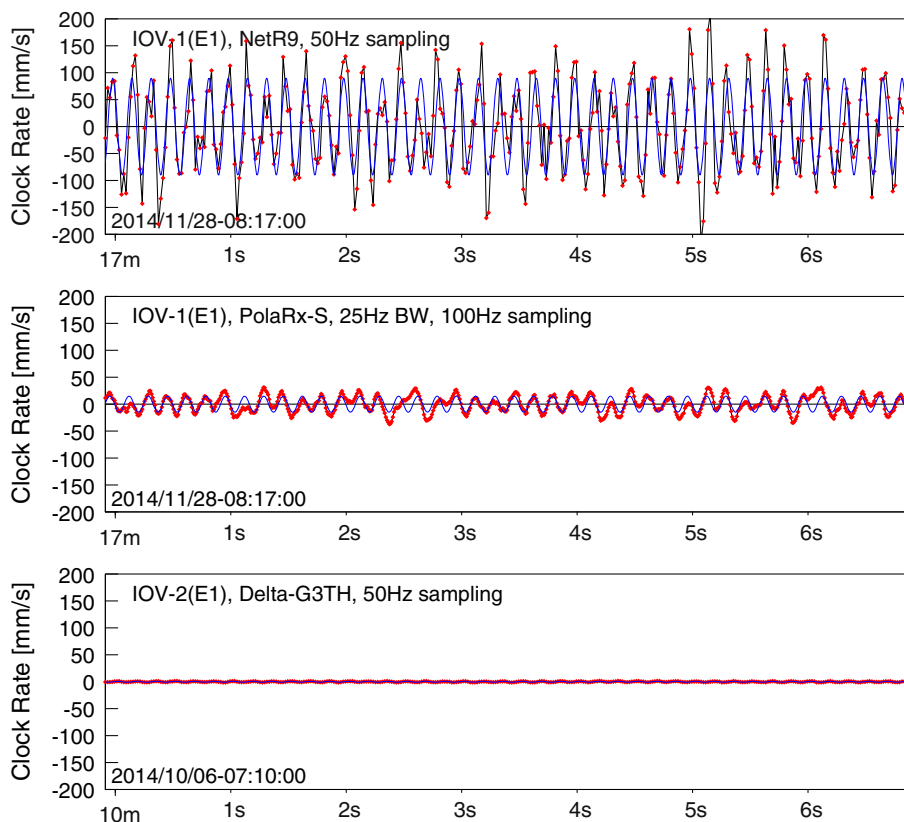

Table 2 Amplitudes of IOV-1/2 clock rate variations for the test cases considered in Table 1

Receiver	B	Rate	IOV-1		IOV-2	
	(Hz)	(sps)	E1	E5a	E1	E5a
NetR9	–	50	8.8	8.8	9.7	9.7
PolaRx-S	15	100	1.0	1.2	1.3	1.4
	25	100	1.5	1.7	1.8	2.1
Delta-G3TH	25	50	–	–	0.1	0.1
Sigma-G3TAJ	25	100	2.7	2.3	2.8	2.4
	25	20			2.9	3.3
GRX1200	15	20			5.4	5.4

All values are given in (cm/s) and exhibit a repeatability for different data intervals of 5 mm/s or better

(2015) will be critically dependent on these algorithms and the specific value of δf.

Low-rate observations in geodetic networks

While the use of high-rate GNSS receivers enables a detailed inspection of the IOV-1/2 clock oscillations, most GNSS receivers in geodetic networks are operated at sampling rates of 1–1/30 Hz. Until the beginning of 2015, an offset close to, but not exactly equal to 6 Hz was configured between the two CMCU synthesizers of both satellites. In case of a perfect commensurability of the receiver sampling interval, which commonly amounts to 1 s or multiples thereof, and the period of the high-frequency clock variation, identical clock variations would be sensed at consecutive measurements epochs. In practice, however, the small offset between the actual oscillation frequency and the nearest integer multiple of 1 Hz causes a beat with a period of the order of several minutes. The "nominal" 5.996 Hz oscillation described above exhibits a 4 mHz offset from 6 Hz, which then results in a beat period $T = 1/4\,\text{Hz} = 250\,\text{s}$ of about 4 min.

As discussed above, the oscillation originates in the master clock signal but impacts the carrier phase observations of different receivers in a different manner due to the specific tracking loop architecture and bandwidth of each receiver. As such, it does *not* cancel in a double-difference (DD) as would typically be the case for low-rate clock variations. This is illustrated in Fig. 8 by DD carrier phase observations of IOV-1 obtained at an MGEX station in Singapore, which comprises two different receiver types connected to a common antenna. In the specific case, a 3-min beat period arises corresponding to a clock oscillation of about 5.995 Hz.
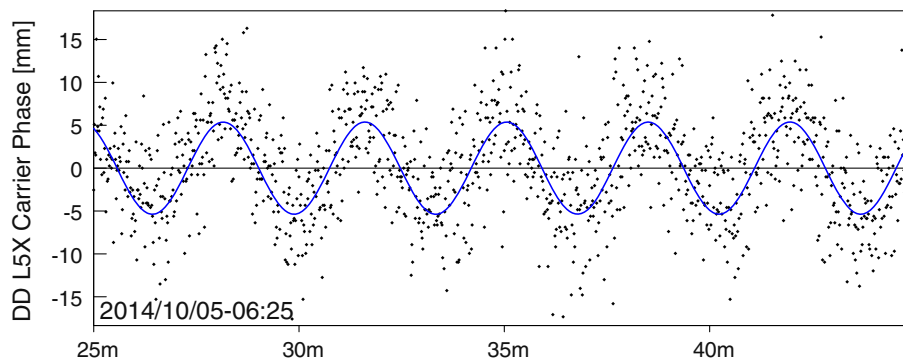
Fig. 8 Example of a 3-min beat period due to high-frequency (5.995 Hz) clock variations of Galileo IOV-1. The *graph* shows double-difference of IOV-1 carrier phase measurements on the E5a frequency relative to the IOV-3 reference satellite as obtained with a Javad Delta-G3TH and a Trimble NetR9 receiver connected to the same antenna (SIN0 and SIN1 stations of the IGS/MGEX network) at 1 Hz sampling rate

The beat period is not constant, though, but has been found to vary over time (Katsigianni 2015). Using DD carrier phase measurements collected at the USN4/USN5 station at the US Naval Observatory in Washington, which hosts a NovAtel OEM6 and a Septentrio PolaRx-T receiver with common antenna, the beat periods shown in Fig. 9 have been derived.

As can be seen, the periods vary between a minimum of about 3 min and a maximum near 13 min for the two satellites during the time 2013–2014. The peak values occurred for a period of several weeks in late August to early September of 2013 and included one of the test dates discussed in Borio et al. (2015). Similar to the higher beat period seen on IOV-2 since early 2015, they relate to the use of rubidium clocks as primary frequency standards. Information on the employed clock is available from information pages at the Galileo Service Center (GSC, http://www.gsc-europa.eu/system-status/Constellation-Information) and can also be inferred from the a_2 coefficient of the clock polynomial in the broadcast navigation message.

Since early January (IOV-1) viz. late March 2015 (IOV-2), obvious periodicities can no longer be seen in the DD carrier phase observations collected at 1- to 30-s sampling. Even though the high-rate measurements collected on March 30, 2014, indicate the continued presence of a cross talk for at least satellite IOV-2, the frequency is no longer near-commensurable with the 1-s sampling and thus creates a noise-like carrier phase variation rather than a clear beat pattern. For IOV-1, in contrast, the impact of cross talk is mitigated by continuous alignment of both synthesizers.

Summary and conclusions

Due to a subtle cross talk in the clock monitoring and control unit of the Galileo IOV-1 and IOV-2 satellites, oscillations of up to a few millimeter amplitude and a
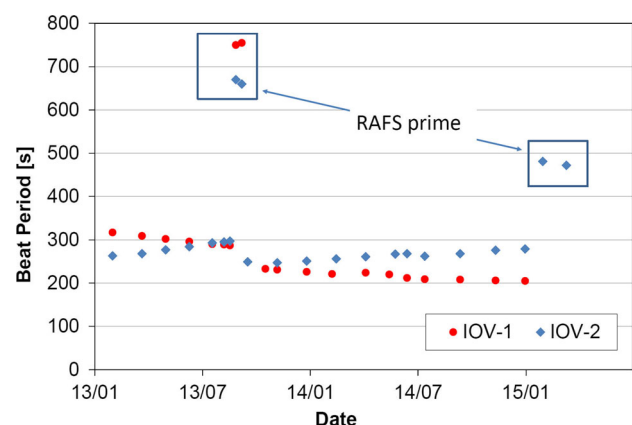

Fig. 9 Beat period of IOV-1/2 clock oscillation at 1 Hz sampling between January 2013 and April 2015

frequency near 6 Hz have occurred until early 2015 in carrier phase measurements of these satellites. No other IOV or FOC satellites have shown similar features, and the problem has largely been mitigated through onboard reconfigurations in the first quarter of 2015.

While the oscillation frequency is much higher than the 1 Hz sampling rate of common GNSS receivers, a close commensurability resulted in comparatively long beat periods of 3–13 min. Even though the oscillation originates from the satellite clock, it does not normally cancel in receiver–receiver differences.

While the received signal is common to all receivers, the resulting measurements differ due the different characteristics of the phase-locked loops (PLL) of the receivers. Since the circular frequency of $2\pi \cdot 6$ Hz is comparable to the bandwidth of the PLL, different amplitudes as well as notable phase shifts of the tracked signal relative to the incoming signal are encountered, which ultimately give rise to the previously discussed errors in the double-difference carrier phase observations. As such, between-

receiver single-differences using different receiver types as well as double-difference measurements involving IOV-1 and IOV-2 will result in small carrier phase oscillations. Even though details of the actual PLL implementations are not publicly disclosed for the employed receivers, the fundamental phenomena can be understood from the discussion of a standard third-order PLL provided here.

"Puzzling" oscillations in double-difference carrier phase measurements have indeed been observed by various researchers in the analysis of zero-baseline tests aiming at a characterization of Galileo receiver measurements, but the issue has also been overlooked in various cases, e.g., Odijk and Teunissen (2013) and Paziewski and Wielgosz (2015) due to a lack of public awareness of the cross talk and its implications.

At a representative level of a few millimeters, the oscillations in the double-difference carrier phase oscillations are typically slightly larger than the noise and multipath level and might thus result in a subtle degradation of differential positioning results conducted in a kinematic mode. Concerning ambiguity resolution over short and long baselines, the oscillation amplitude appears small enough compared to the wavelength to have no adverse impact on ambiguity resolution rates. However, further analyses would be required to substantiate this assumption.

Static surveys averaging over time intervals sufficiently long, compared to the 4-min beat period, are likely to be unaffected by the oscillations. Similar considerations apply for the precise orbit determination of the Galileo IOV satellites which is essentially insensitive to periodic measurement variations at a timescale much smaller than the orbital period. On the other hand, the estimated satellite clock offset values would directly be affected by the different response of the employed receivers. In particular, Allan deviations derived from one-way carrier phase measurements (Gonzalez and Waller 2007; Hauschild et al. 2013; Griggs et al. 2015) would potentially show a small increase at half the beat frequency, i.e., approximately 2 min, rather than the native clock stability.

In addition to different tracking loop implementations, different concepts are also employed by the various receivers for forming range-rate (Doppler) observations from time-differenced carrier phases. Depending on the employed approach, receivers may either filter out the rapid carrier oscillation or show a periodic Doppler error well above the usual noise level.

As of early 2015, the IOV-1/2 CMCUs have been reconfigured and the clock oscillation is no longer present in IOV-1 due to an active alignment of the synthesizers. For IOV-2, which has since then been using rubidium clocks, an oscillation with a 12.6 Hz frequency could still be sensed with some receivers of appropriately high sampling rate and PLL bandwidth.

Beyond the characterization of the IOV-1/2 satellites themselves, the presented results are of interest for the characterization of high-rate GNSS receivers, which are used in diverse applications such as the monitoring of scintillation, structural deformation or earthquakes. The 6 Hz carrier oscillation experienced by the IOV-1/2 satellites in 2013 and 2014 has provided a unique opportunity for studying the response of geodetic receivers to rapid phase variations. The availability of a signal in space with known variations has helped to gain a better understanding of the receiver-specific phase and Doppler measurement properties for such receivers and complements traditional test concepts such as forced antenna oscillations (Moschas and Stiros 2014; Häberling et al. 2015).

References

Borio D, Gioia C, Mitchison N (2015) Identifying a low-frequency Oscillation in Galileo IOV pseudorange rates. GPS Solut. doi:10.1007/s10291-015-0443-7

Carrillo FJM, Sanchez AA, Alonso LB (2005) Hybrid synthesizers in space: Galileo's CMCU. In: Proceedings of 2nd international conference on recent advances in space technologies, IEEE, pp 361–368

Felbach D, Heimbuerger D, Herre P, Rastetter P (2003) Galileo payload 10.23 MHz master clock generation with a clock monitoring and control unit (CMCU). In: Proceedings of IEEE 2003 frequency control symposium and 17th European frequency and time forum, pp 583–586. doi:10.1109/FREQ.2003.1275156

Felbach D, Soualle F, Stopfkuchen L, Zenzinger A (2010) Clock monitoring and control units for navigation satellites. In: Proceedings of IEEE 2010 frequency control symposium (FCS), IEEE, pp 474–479. doi:10.1109/FREQ.2010.5556283

Gonzalez F, Waller P (2007) Short term GNSS clock characterization using one-way carrier phase. In: IEEE international FCS 2007 and 21st EFTF, pp 517–522. doi:10.1109/FREQ.2007.4319127

Griggs E, Kursinski E, Akos D (2015) Short-term GNSS satellite clock stability. Radio Sci 50(8):813–826. doi:10.1002/2015RS005667

Häberling S, Rothacher M, Zhang Y, Clinton JF, Geiger A (2015) Assessment of high-rate GPS using a single-axis shake table. J Geodesy 89(7):697–709. doi:10.1007/s00190-015-0808-2

Hauschild A, Montenbruck O, Steigenberger P (2013) Short-term analysis of GNSS clocks. GPS Solut 17(3):295–307. doi:10.1007/s10291-012-0278-4

Katsigianni G (2015) Zero-baseline analysis of Galileo data from multi-GNSS experiment. Master's Thesis, Technische Universität München

Montenbruck O, Steigenberger P, Khachikyan R, Weber G, Langley RB, Mervart L, Hugentobler U (2014) IGSMGEX: preparing the ground for multi-constellation GNSS science. Inside GNSS 9(1):42–49

Moschas F, Stiros S (2014) PLL bandwidth and noise in 100 Hz GPS measurements. GPS Solut 19(2):173–185. doi:10.1007/s10291-014-0378-4

Odijk D, Teunissen PJ (2013) Estimation of differential inter-system biases between the overlapping frequencies of GPS, Galileo, BeiDou and QZSS. In: 4th international colloquium scientific and fundamental aspects of the Galileo programme, pp 1–8, 4–6 December 2013, Prague

Paziewski J, Wielgosz P (2015) Accounting for Galileo-GPS inter-system biases in precise satellite positioning. J Geodesy 89(1):81–93. doi:10.1007/s00190-014-0763-3

Ward PW, Betz JW, Hegarty CJ (2006) Satellite signal acquisition, tracking, and data demodulation. In: Kaplan ED (ed) Understanding GPS—principles and applications, chap 5. Artech House, Boston, pp 174–175

Oliver Montenbruck is the head of the GNSS Technology and Navigation Group at DLR's German Space Operations Center. His research activities comprise space-borne GNSS, precise orbit determination as well as new GNSS signals and constellations. He chairs the Multi-GNSS Working Group of the International GPS Service and serves as a lecturer at Technische Universität München.

André Hauschild is a member of the scientific staff of the GPS Technology and Navigation Group at DLR's German Space Operations Center (GSOC). His field of work focuses on real-time precise clock estimation for GNSS satellites as well as multi-GNSS processing using modernized GPS and new satellite navigation systems. He is also involved in projects with space-borne GNSS receivers for scientific applications like precise orbit determination and radio occultation.

Simon Häberling received a master degree in Geodesy from the ETH Zurich. He is currently working as a PhD student in the field of high-rate GNSS, especially for seismological applications.

Benjamin Braun is a member of the GNSS Technology and Navigation Group at DLR's German Space Operations Center since 2013. He is working on hybrid navigation systems for sounding rocket and launch vehicle applications comprising inertial sensors and GNSS receivers. His research is particularly focused on increasing the robustness of GNSS by inertial aiding.

Gina Katsigianni received her diploma in Surveying Engineering and a master degree in Geoinformatics from National Technical University of Athens. She analyzed the Galileo IOV-1/2 clock variations for her master thesis in the Earth-Oriented Space Science and Technology program at Technische Universität München. She is now working as young graduate trainee at the European Space Agency.

Urs Hugentobler is professor for satellite geodesy at the Technische Universität München, Germany, and head of the Research Facility Satellite Geodesy. His research activities include precise positioning using GNSS, precise orbit determination and modeling, reference frame realization, clock modeling and time transfer, involving the new satellite systems.